Processing and Characterization of Functionally Graded Aluminum (A319)—SiC$_p$ Metallic Composites by Centrifugal Casting Technique

E. JAYAKUMAR, JIBIN C. JACOB, T.P.D. RAJAN, M.A. JOSEPH, and B.C. PAI

Functionally graded materials (FGM) are successfully adopted for the design and fabrication of engineering components with location-specific properties. The present study describes the processing and characterization of A319 Aluminum functionally graded metal matrix composites (FGMMC) with 10 and 15 wt pct SiC$_p$ reinforcements. The liquid stir casting method is used for composite melt preparation followed by FGMMC formation by vertical centrifugal casting method. The process parameters used are the mold preheating temperature of 523 K (250 °C), melt pouring temperature of 1013 K (740 °C), and mold rotation speed of 1300 rpm. The study analyzes the distribution and concentration of reinforcement particles in the radial direction of the FGMMC disk along with the effects of gradation on density, hardness, mechanical strength, the variation in coefficient of thermal expansion and the wear resistance properties at different zones. Microstructures of FGMMC reveal an outward radial gradient distribution of reinforcements forming different zones. Namely, matrix-rich inner, transition, particles-rich outer, and chill zone of a few millimeters thick at the outer most periphery of the casting are formed. From 10-FGM, a radial shift in the position of SiC$_p$ maxima is observed in 15-FGM casting. The mechanical characterization depicts enhanced properties for the particle-rich zone. The hardness shows a graded nature in correlation with particle concentration and a maximum of 94.4 HRB has been obtained at the particle-rich region of 15-FGM. In the particle-rich zone, the lowest CTE value of 20.1 μm/mK is also observed with a compressive strength of 650 MPa and an ultimate tensile strength of 279 MPa. The wear resistance is higher at the particle-rich zone of the FGMMC.

© The Minerals, Metals & Materials Society and ASM International 2016

I. INTRODUCTION

ALUMINUM-SILICON-BASED alloys, due to their high strength to weight ratio, have received a considerable attention in the various mechanical manufacturing sectors. The weight reduction in the components of aerospace and automobiles leads to a significant impact on the fuel economy.[1] A319, A356, and A390 alloys are well suited for wear-resistant and weight critical applications such as brake drums, cylinder liners, pistons, cylinder blocks, connecting rods, and clutch housing in automobiles. Silicon-based aluminum alloys are used in helicopter structural parts such as parts of the body, support for rotor plates, and drive shafts. They are also suitable for producing rotor vanes in compressors and aero-engines.[2] Functionally graded materials (FGM) are a class of advanced composite materials consisting of two or more phases, with variation in composition and/or microstructure in spatial direction. FGMs can be processed to obtain higher superficial hardness with adequate internal toughness properties that are not attainable by a monolithic or a homogeneous material.[3] The gradation reduces the local stress concentration, thermal and residual stresses, which are commonly experienced in traditional composites. Gradation can also modify the location-specific mechanical and thermal properties, with a proper combination of different matrices and reinforcements with suitable properties, size and/or shape. A metal matrix FGM with ceramic reinforcements can provide a single material with good thermal protection and load carrying capability thereby eliminating the possibility of cracking and spalling of tiles that are experienced in the Space Shuttle outer surfaces.[4–8] Even though FGMs developments started as thermal barrier materials for aerospace structural applications and fusion reactors, now they are strongly considered as a potential structural material for the design of high-speed aerospace vehicles and for components in the high-temperature environments. Light-weight composite airframes can also increase the payload capacity, speed, range, and endurance. The properties of composites are greatly influenced by the type of reinforcement particles, size of particles, and its volume fraction. The industrial interest in FGMs is mainly related with the opportunity of

E. JAYAKUMAR, Research Scholar, T.P.D. RAJAN, Senior Scientist, and B.C. PAI, Emeritus Scientist, are with CSIR - National Institute for Interdisciplinary Science and Technology, Thiruvananthapuram 695019, Kerala, India. Contact e-mail: tpdrajan@rediffmail.com JIBIN C JACOB, M.Tech. Student, and M.A. JOSEPH, Professor, are with the National Institute of Technology, Calicut 673601, Kerala, India.

controlling the gradation of the physical and/or chemical properties, through microstructural manipulation. By centrifugal casting method, the volume of reinforcement addition and its radial distribution can be controlled to produce components with better thermal dimensional stability and more wear resistance properties. The A319 exhibits good casting qualities including pressure tightness, moderate strength, good weldability, and corrosion resistance. In the automobiles components like the brake discs, liners, and pistons, only the rubbing surfaces or the contact regions require more wear resistance property and the other portions can be less populated or even reinforcement free.[9] The FGM formation with SiC_p reinforcements with location-specific wear-resistant properties leads to increased component service life due to the minimum wear and tear. In the case of automobile pistons and cylinder liners, in addition to the external reinforcement additions, better thermal and mechanical properties can also be achieved by the second-phase gradations like the gradation of in situ primary silicon.[10,11]

The reinforcements can be introduced into the MMC melt by ex situ and in situ methods of preparations. In the in situ composite preparations, the reinforcements like, TiB_2, TiC, and AlB_2, are formed by reactions that are occurring during the processing.[12,13] By suitably setting the process parameters, the sizes of the reinforcements and their homogeneity in distribution can be well controlled. The clean interfaces of fresh reinforcements increase their wettability with the matrix.[14] FGMMC with graded properties can also be prepared by the ex situ additions with Al_2O_3, TiB_2, TiO_2, SiC, TiC, B_4C, graphite and SiC particles. The lower wettability problems arise in ex situ additions due to the presence of oxide films on the surface of molten metal and the adsorbed contaminant on the reinforcements can be well controlled either by metallic coatings or heat treatment of reinforcement particles and by the addition of smaller percentages of reactive elements, like magnesium, calcium or titanium, to the molten metal during processing.[15–18]

Centrifugal casting is one of the simple pressure die casting methods by which FGMs can be manufactured economically. An increased centrifugal force is applied to the melt containing reinforcement particles or phases by pouring the melt into the rotating molds and thereby forming different zones of reinforcement concentrations during solidification. The extent of particle concentration, relative locations, and the zonal sizes within the casting are mainly controlled by the melt temperature, melt viscosity, cooling rate, the densities of the particles, and the matrix. The particle size, the initial volume of addition during the melt preparation, and magnitude of centrifugal acceleration determine the magnitude and the position of maximum concentration point.[19,20]

The present study describes the processing of A319 Aluminum functionally graded metal matrix composites reinforced with 10 wt pct and 15 wt pct SiC_p of average particle size of 23 μm. The two different concentrations of reinforcements are selected in such a way that the variations are clearly visible during the characterizations. Addition of less percentages of

particles will not yield a significant improvement in properties, while, on the other hand, very high percentage additions of SiC_p leads to difficulty in getting a good MMC melt with neat dispersion due to the high viscosity and increased particle agglomeration tendency. Liquid metal stir casting method is adopted for the composite preparation and FGMMC castings are produced by vertical centrifugal casting technique. Mechanical and tribological characterizations have been carried out. The main objective of this work is to evaluate gradation, distribution, and the influence of SiC particles at different locations on the behavior of mechanical properties of functionally graded aluminum metal matrix composites.

II. MATERIALS AND METHODS

Hypoeutectic, A319, Al-Si alloy was used for the preparation of the composite. The chemical composition (refer Table I) is 88.83 pct of Aluminum with 6.35 pct of Si and 3.87 pct of Cu as major alloying elements and less than 0.2 pct minor alloying elements. The SiC particles of density 3.2 g/cm^3 with an average particle size of 23 μm are used as reinforcements. The FGM composites were made by two steps: Preparation of homogeneous composite melt of desired composition by liquid metal stir casting technique, followed by, pouring the melt into a rotating metal mold which is fitted to the shaft of a vertical centrifugal casting machine.

The composite melt synthesis was carried out in a 10-kg capacity annealed clay graphite crucible in an electrical-resistance furnace. The cleaned SiC_p were preheated and added to the steady vortex at a controlled feed rate at a melt temperature of 1003 K to 1013 K (730 °C to 740 °C). Selection of 10 and 15 wt pct SiC_p was chosen to obtain the best dispersion in order to get a consistent MMC melt and good gradations in the properties of casted FGMMCs. The steady vortex was maintained by a hydro-drive dynamometer with a graphite-coated mild steel stirrer rotating at a speed of around 250 rpm.[21,22] After the completion of powder addition, the stirring is continued for 20 minutes and stopped. A baffle is introduced into the melt for consistency and uniform mixing of the composite and then stirring was restarted, continued for another 15 more minutes at 1033 K (760 °C). The crucible was taken out of the furnace; in order to remove any slag or dirt particles, a thin layer from the top of the melt was skimmed off. Hand stirred and a portion of the melt were poured at 993 K (720 °C) to the preheated [523 K (250 °C)] gravity die casting molds for homogeneous composite cast specimens for reference. A circular disk-shaped mold of dimension 300 mm diameter and a thickness of 28 mm were used for FGMMC cast preparations. The mold was preheated to a temperature of 523 K (250 °C) for 2 hours. Just before pouring, the mold was transferred from the preheating furnace, fixed on the shaft of the vertical centrifugal casting machine and kept in rotation with a speed of 1300 rpm. At a melt temperature of 1013 K (740 °C), with the help of a pouring cup, MMC melt was uniformly and steadily

Table I. Chemical Composition of A319 Alloy

Details of Alloy	Major Alloying Elements in Percentage		Minor Alloying Elements in Percentage						Al in Percentage Al (Balance)
	Si	Cu	Mg	Fe	Mn	Zn	Ni	Ti	
A319 as per standards	5.5 to 6.5	3.0 to 4.0	0.10	1.00	0.50	1.00	0.35	0.25	86.3 to 91.5
A319 ingot	6.35	3.87	0.072	0.205	0.34	0.148	0.046	0.14	88.83

poured into the rotating mold to obtain FGMMC castings.

After cooling, the castings are removed from the molds and cleaned. A319 is a precipitation hardening alloy and the standard T6 condition heat treatment procedure followed is as described: solution heat treatment for 8 hours at 778 K (505 °C) followed by quenching at 353 K (80 °C) hot water then precipitation or age hardened at 428 K (155 °C) for 5 hours.[23] SPECTRO MAXX optical emission spectrometer was used to find out chemical composition of base alloy. DMRX Leica optical microscope was used to capture the microstructures and Leica Qwin image analyser was used for the calculation of volume percentage of SiC_p distribution along the radial direction. The density was determined by using Archimedes principle method. Hardness in HRB scale was tested by FIE (TWIN) Rockwell hardness tester with a hardened steel ball indenter of 1/16″ diameter for an applied load of 100 kgf for 15 seconds. SII SS/7300 Thermo mechanical analyzer was used for the CTE measurements. INSTRON 1195-5500R series tensile and compression tester was used for the tensile and compression testing. Dry wear tests were conducted on an EN31 hardened steel disk in a DUCOM (LR20E) pin on disk tribometer with heat-treated FGMMC pins of diameter 6 mm with a length of 30 mm. Each wear test was conducted with a relative velocity of 2 m/s for a sliding distance of 1800 m. ZEISS stereo microscope was used to take macrographs of the worn-out pin ends for surface morphology studies, and JEOL Scanning Electron Microscope images were used to understand the nature of wear.

III. RESULTS AND DISCUSSION

Figure 1(a) shows the optical micrographs of the gravity cast A319 aluminum alloy. The dark needle like eutectic silicon phases, the gray $CuAl_2$ phase and white α-Al matrix phases are observed.[24] Evenly spaced secondary dendritic arms are visible in the microstructure. Figures 1 (b) and (c) show the optical micrograph of 10 and 15 wt pct SiC gravity castings in the as-cast condition. The micrograph of composite depicts uniform distribution of silicon carbide particles (dark) in Aluminum alloy matrix.

Figure 1(d) shows the schematic diagram of a centrifugally cast FGMMC disk with observed zones and locations, from where test specimens are prepared for microstructure, hardness, density, tensile, compression, and wear analysis. Figures 2 and 3 show the optical micrographs of centrifugally cast A319-10 wt pct SiC_p FGMMC disk (10-FGM) and 15wt pct SiC_p FGMMC (15-FGM) taken from inner towards outer in the radially outward direction respectively. In both, four microstructure regions are observed and namely they are: the matrix-rich zone (the inner region which is free from the reinforcement particles), the transition, particle-rich, and the chilled zone (the outer most periphery of the disc). For the completion solidification, a cast disk of diameter 300 mm and thickness 28 mm will take about 2 to 3 minutes. The solidification process (solidification front) in a centrifugal casting is a directional one and is from outer most periphery of the mold towards the inner diameter of the casting i.e., radially inward direction, while the denser reinforcement particles and secondary phases will diffuse from inner towards outer diameters (diffusion front) due to the centrifugal force i.e., radially outward direction. The position of the particle-rich zone, size, and the maximum value of particle concentration depends on the solidification time and the centrifugal force (G effect). Even though there is the chilled zone, of size 2 to 3 mm radial, oppositely moving solidification front and the particle diffusion fronts will meet outside the chilled zone and this radial position will determine the exact location and magnitude of maximum particle concentration. The specific heat capacity of SiC_p (1300 J kg^{-1} K^{-1}) is higher than that of the aluminum matrix alloy (963 J kg^{-1} K^{-1} in liquid state and 1084 J kg^{-1} K^{-1} solid state). Hence the composite with higher volume fraction SiC_p has more heat content to release, leading to longer solidification time enabling more particle diffusion towards outer periphery. The maximum particle concentration position was observed near at 55 mm for 10-FGM with 18.5 wt pct of SiC_p and near at 75 mm for 15-FGM with 28 wt pct of SiC_p from inner diameter of the casting towards the outer diameter in the radial direction. Figures 2(a) and 3(a) show the inner matrix-rich zone/powder depleted region of average zone size 25 to 30 mm radial thickness. In both microstructures only α-Al and eutectic Al-Si phases are visible. Very few particles are being observed in the near vicinity of transition zones. Towards the inner most diameters, the microstructures show gas porosity and particle agglomerations (not shown). In the case of a real application, those inner most regions can be properly machined off during the finishing operations. Figures 2(b) and 3(b) show the transition zone of average zone size 20 mm radial thicknesses. Clear variations in particle concentrations are observed in the transition zone microstructures. Figures 2(c) and 3(c) show the particle-rich zone (average zone size 25 to
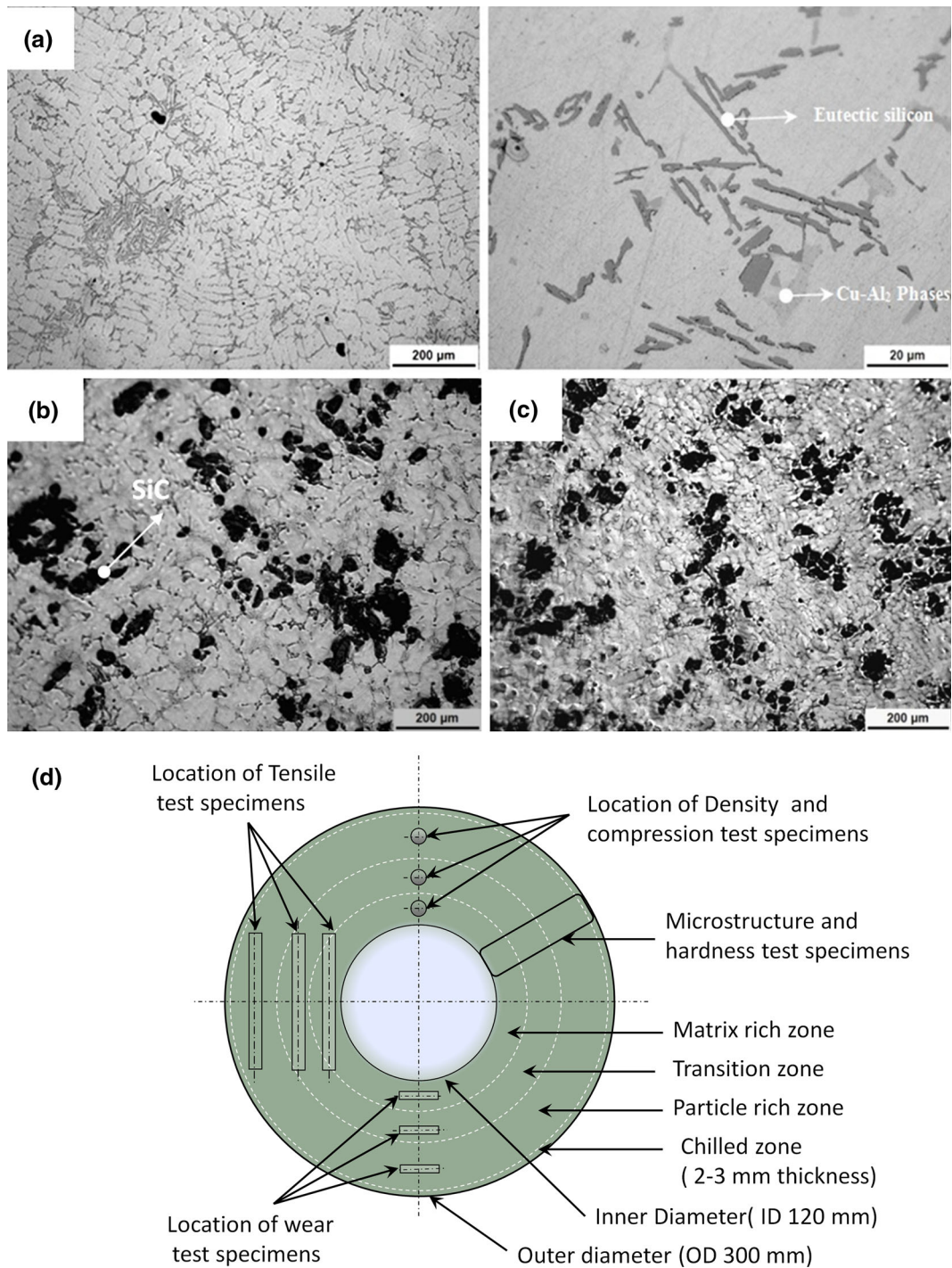
Fig. 1—Microstructures of gravity cast (*a*) A319 alloy, (*b*) A319-10 pct SiC MMC, and (*c*) A319-15 pct SiC MMC (*d*) Schematic diagram of the casting with observed zones and location of specimens prepared for characterizations.

40 mm radial thickness). The outer most periphery/chilled zone has an average zone size of 2 to 3 mm radial thickness with less particle concentration compared to the adjacent region. This is due to the immediate solidification of the liquid composite melt which comes in contact with the mold surface. The region near outer with higher concentration of particles, near inner with a depletion of particles, and the connecting transition region in the middle with a less and varying concentrations of reinforcement particles clearly constitute a graded microstructure. Figures 4(a) through (c) show the microstructures of A319 base centrifugal casting taken from similar radial positions that of FGMMC castings. Since A319 is a hypoeutectic alloy (Al 6Si 3.5Cu), gradation in primary silicon particles is not observed in the microstructure. Due to the higher
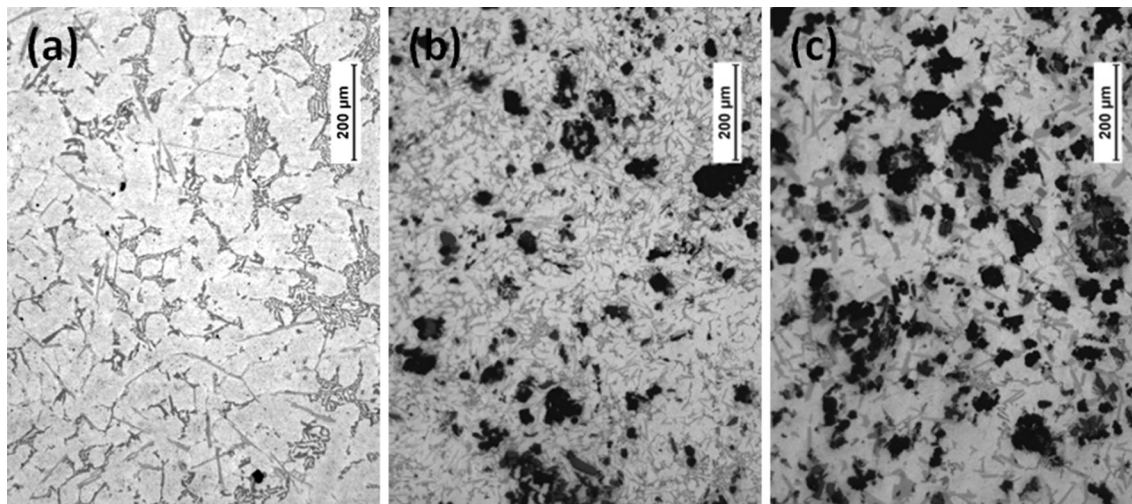
Fig. 2—Microstructures of 10-FGM from inner to the outer periphery of the casting (a) Inner matrix-rich zone/powder-depleted region (average zone size 25 to 30 mm radial thickness), (b) Transition zone (average zone size 20 mm radial thickness), (c) Particle-rich zone (average zone size 25 to 40 mm radial thickness).
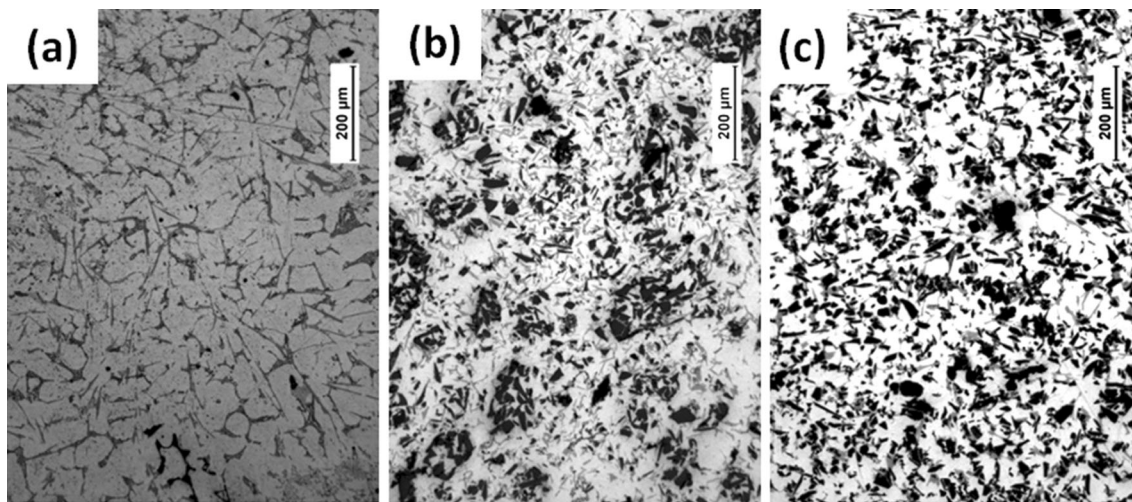

Fig. 3—Microstructures of 15-FGM from the inner to outer periphery of the casting (a) Inner matrix-rich zone/powder-depleted region (average zone size 25 to 30 mm radial thickness), (b) Transition zone (20 mm), (c) Particle-rich zone (25 to 40 mm).

solidification rate, the grain size of the primary aluminum (α-Al) and eutectic silicon phases are finer towards the outer periphery. Both the inward solidification and the outward centrifugal forces sweep the light weight agglomerated reinforcements and segregated gas porosities towards the inner periphery of the casting and produces a clean dense porous-free regions of microstructures throughout the castings.

Figure 5 shows the densities of the homogeneous gravity cast composites and that of FGMMC specimens taken from different zones located at distances of 30, 55, and 75 mm from inner towards outer. The density value of homogeneous gravity cast A319-10 SiC_p is 2.756 g/cm^3 and that of A319-15 SiC_p is 2.789 g/cm^3. Both the composites show similar behaviors in density variations. In the case of matrix-rich region, specimens (from 30 mm) clearly show lesser density value of 2.754 and 2.742 g/cm^3, respectively, and are due to the absence of

denser SiC particles. The density of both FGMMC specimens taken from the particle-rich regions is high as expected due to the presence of maximum percentages of particles, and the respective values of 10-FGM and 15-FGM are 2.83 g/cm^3 (at 55 mm) and 2.87 g/cm^3 (at 75 mm). Figure 6 shows that the volume percentage distribution of SiC_p in radial direction is calculated by image analysis from inner to outer diameter of the casting. For 10-FGM, the maximum concentration is observed at a distance of near 55 mm from the inner towards the outer diameter and the maximum point, for 15-FGM, is obtained at near 75 mm from the inner diameter. There is an outward shift in position of maxima in the case of 15-FGM. The calculations closely follow the experimental values of density and support the hardness values obtained from the similar locations of the FGM specimens. Table II shows the Rockwell hardness (HRB) of gravity-casted alloy and the
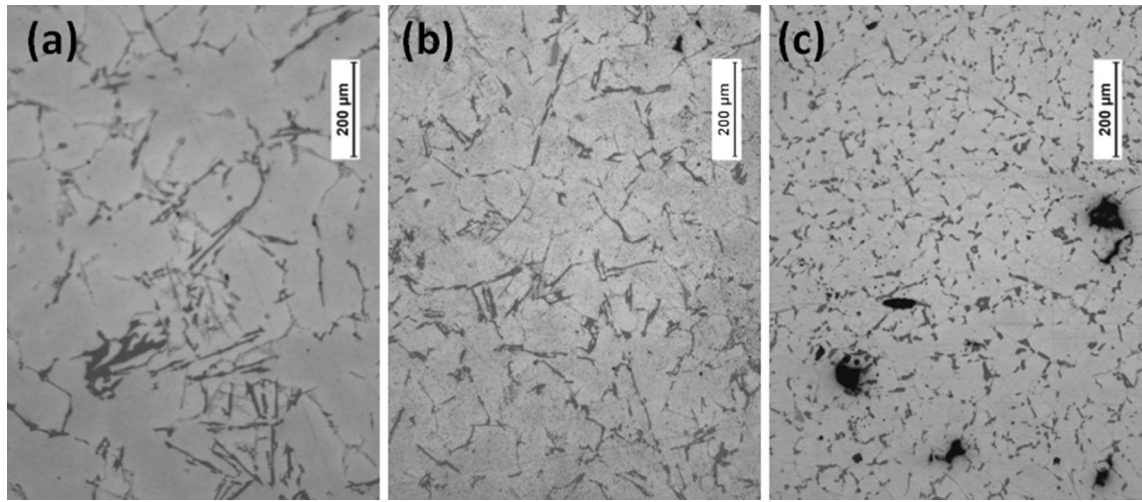
Fig. 4—Microstructures of A319 base centrifugal casting from the inner to outer periphery. Microstructures (*a*), (*b*), and (*c*) are taken from similar radial positions that of FGM castings.
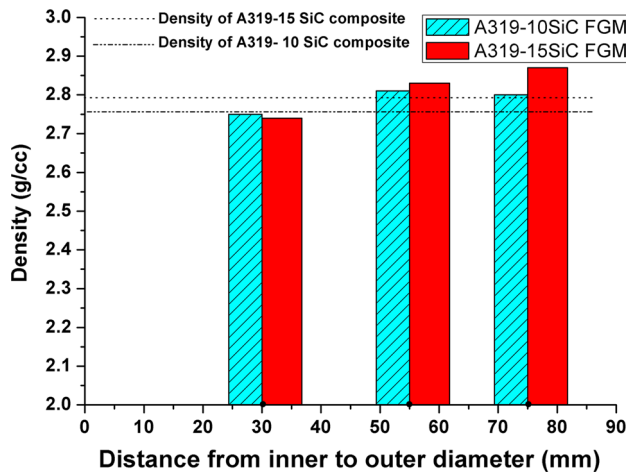

Fig. 5—Density of both 10-FGM and 15-FGM castings at a distance of 30, 55, and 75 mm from inner towards outer diameter of the casting.
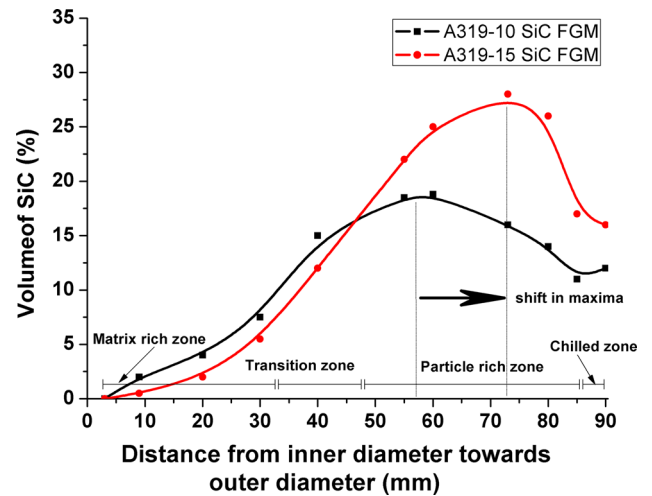

Fig. 6—Volume percentage distribution of SiC reinforcements in radial direction of both 10-FGM and 15-FGM castings from inner towards outer diameter of the casting.

composites before and after heat treatments. Hardness variations along the radial direction of as-cast as well as the heat-treated samples of 10-FGM are shown in Figure 7(a) and that of 15-FGM are shown in Figure 7(b). It is observed that the location-wise changes in density values at different zones of FGMMCs closely follow the variations in hardness value suggesting the influence of SiC_p concentrations. Heat treatment improves the hardness as well as other mechanical properties due to the redistribution of $CuAl_2$ phases.[25] It is observed that in all the centrifugal cast FGMMC, the hardness value increases from very low values in the inner periphery, due to porosity, to a maximum in the particle-rich zones and then decreases to a normal value towards the chilled zone of the casting. The hardness values of the heat-treated samples are higher than that of as-cast samples. In Figure 7(a), the maximum hardness of 87 HRB is observed between 45 and 55 mm, and in Figure 7(b) the value of 94.4

HRB is observed between 65 and 75 mm. This shows that the SiC_p impart strength and hardness to the zones in which they are present. The hardness values at the point where iron intermetallic is seen have combined effects of concentration of SiC_p and Al_5FeSi.[26,27] Al_5FeSi is found in the transition zone towards inner region and they are formed due to the iron diffusion from the mild steel stirrers that are used during the melt preparation process.

Figure 8 shows the CTE value taken on both FGMMCs at different zones, and it is clearly seen that the increase in the amount of SiC_p has a major role in the CTE value of the composites. When MMCs cool, misfit strains set in due to the large difference between the coefficients of thermal expansion (CTE) of the matrix and the reinforcements. The thermal stresses induced by the misfit strains increase the dislocation density by creating new dislocations. The rule of
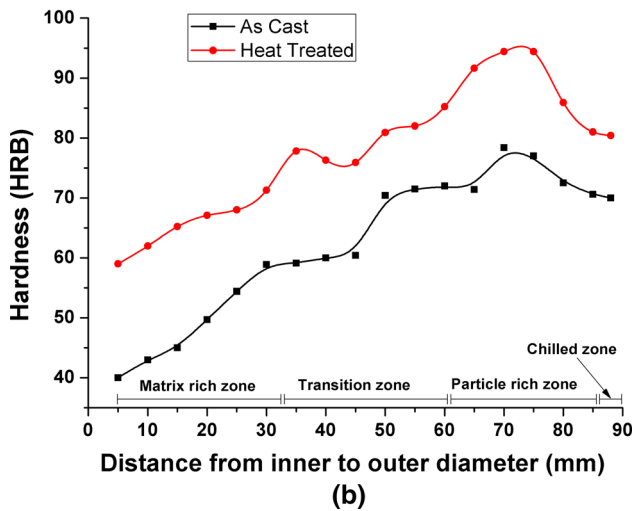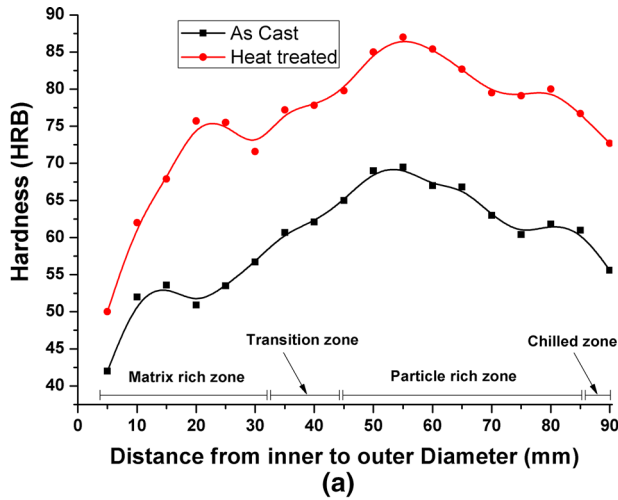
(a)

(b)

Fig. 7—Hardness variation from the inner diameter of the ring towards the outer diameter regions of FGMMC rings in both as-cast and after T6 heat treatment conditions. (*a*) 10-FGM and (*b*) 15-FGM.
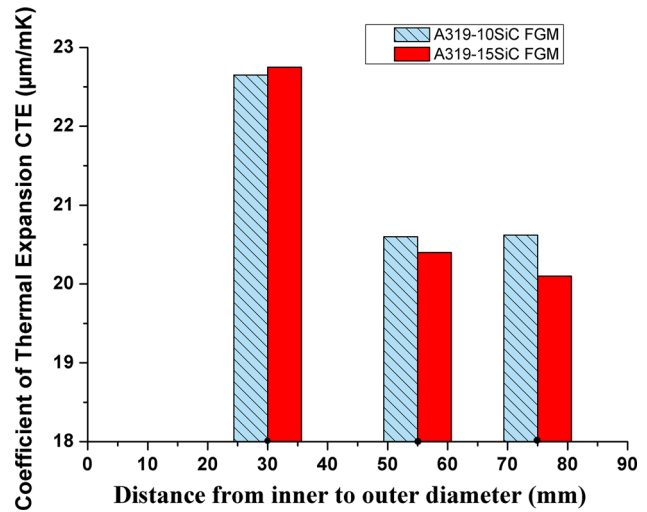

Fig. 8—CTE of 10-FGM and 15-FGM castings measured at three regions (namely matrix-rich, transition, and particle-rich outer regions at a distance of 30, 55, and 75 mm, respectively, from inner towards outer diameter of the casting.).

Table III. Coefficient of Thermal Expansion (CTE) Value of Homogenous Gravity Castings and SiC Particle for the Temperature Range 303 K to 573 K (30 °C to 300 °C)

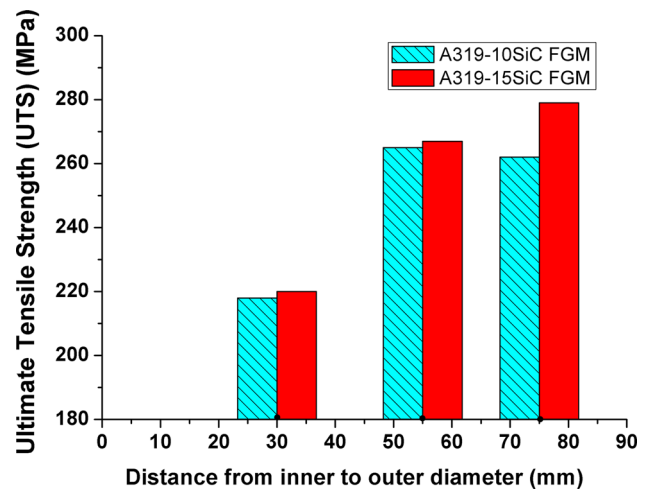| CTE μm/mK	A319 alloy	SiC$_p$	A319-10SiC Composite	A319-15SiC Com posite
Range 303 K to 573 K (30 °C to 300 °C)	22.9	2.77	22.6	20.7

Fig. 9—Ultimate Tensile Strength (UTS) of 10-FGM and 15-FGM castings measured at a distance of 30, 55, and 75 mm, respectively, from inner towards outer diameter of the casting.

mixtures holds well only when the CTE and the elastic properties of the matrix and the reinforcement are the same or comparable. Therefore, an understanding of the CTE of the FGMs is very essential for practical applications. The CTE values of A319 alloy, SiC$_p$, and the MMC in gravity cast conditions are given in Table III. The high concentration of SiC$_p$ reinforcements in particle-rich zone yields low value of CTE and good thermal stability to that region. The grain refinement effects also lower the CTE value of the outer region of 10-FGM to 20.62 μm/mK. The lowest CTE value of 20.1 μm/mK has been obtained for the 15-FGM specimen at 75 mm.
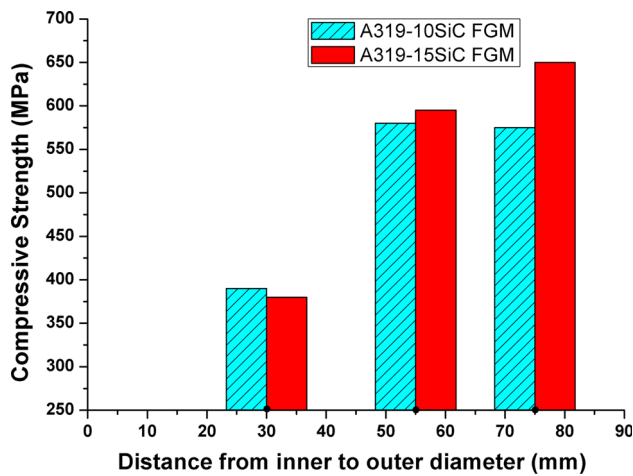
Fig. 10—Compressive strength of 10-FGM and 15-FGMs measured at a distance of 30, 55, and 75 mm, respectively, from inner towards outer diameter of the casting.
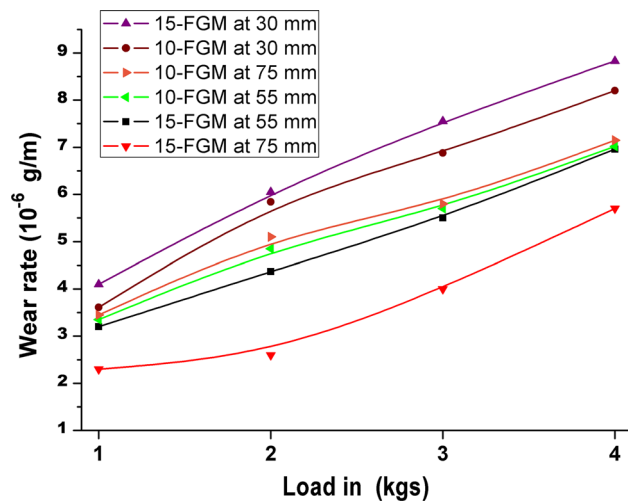

Fig. 11—Wear rate of 10-FGM and 15-FGM heat-treated pins taken from three regions of 30, 55, and 75 mm, respectively, from inner towards outer diameter.

The ultimate tensile strength (UTS) of the A319 base alloy is 230 MPa, and that of the gravity casting of the composites with 10 and 15 pct SiC_p is 257 and 262 MPa, respectively. The presence of SiC_p on the aluminum matrix decreases elongation resulting reduced ductility, and hence, during testing the brittle failure mode occurs. Figure 9 shows the UTS values of specimens taken from the FGMMC rings at distances of 30, 55, and 75 mm in the radial outer direction. For 15-FGM, the UTS value was minimum 220 MPa at 30 mm which is lesser than that of A319 base alloy itself. Then the UTS value increases to 267 MPa at 55 mm due to more SiC_p concentration (approx. 22 pct) and the maximum value of 279 MPa was obtained at the particle-rich zone (at 75 mm with 28 pct SiC_p concentration). In the case of 10-FGM, UTS values are 218, 265, and 262 MPa at 30, 55, and 75 mm, respectively. At 75 mm, the grain refinement effect enhances the UTS values of 10-FGM which is closer to the maximum value. Figure 10 shows the compressive strength values obtained for specimens taken from same locations. They also follow the similar trend of UTS values, indicating that the properties are high at particle-rich zone and are very much sensitive with concentrations of SiC_p.

Dry wear tests are conducted using pin on disk tribometer with heat-treated FGMMC pins taken from the same radial locations FGMMC rings (i.e., at 30, 55, and 75 mm). The test is repeated for four different loads (1, 2, 3, and 4 kg). The wear rates are calculated in terms of weight loss and are plotted in Figure 11. At lower loads, 15-FGM outer pin at 75 mm shows minimum wear loss, and as loading increases, the slope of wear curve changes rapidly and loss increases. For 10-FGM, pins at 55 mm show that lesser wear rate is observed (but higher than that of 15-FGM pin from particle-rich zone at 75 mm) without any sharp transition regions. The pin of 15-FGM at 55 mm shows lesser wear rate than particle-rich pin at 55 mm of 10-FGM due to more SiC_p concentration and grain refinement. The outer pin at 75 mm of 10-FGM very closely follows the above two curves at higher loads. The pins from inner zones have high wear rate due to the direct contact of base alloy with EN 31 wear disk and the rate is proportional to the applied loads. The worn-out surfaces morphology stereo micrographs of FGMMC pins from inner and outer
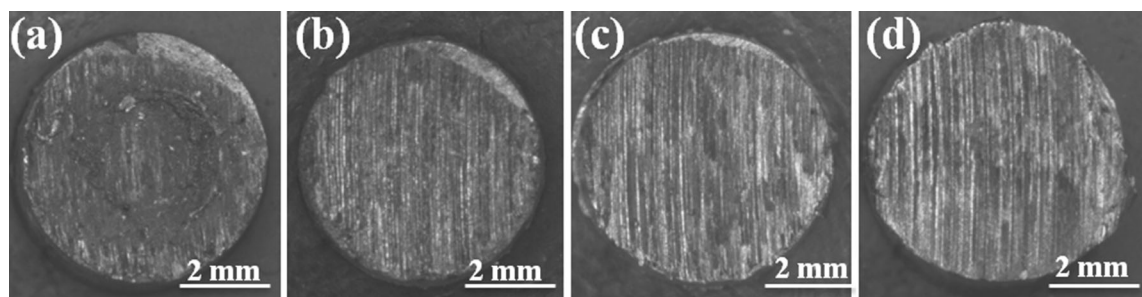

Fig. 12—Stereo micrographs of wear pins (of size 6 mm diameter) worn-out surface of 10-FGM and 15-FGM from different regions at the maximum 4 kg load condition. Wear pins are made from regions namely from (a) 10-FGM ring inner zone at 30 mm (b) 10- FGM ring particle-rich zone at 55 mm (c) 15-FGM ring inner zone at 30 mm (d) 15-FGM ring outer zone at 75 mm.
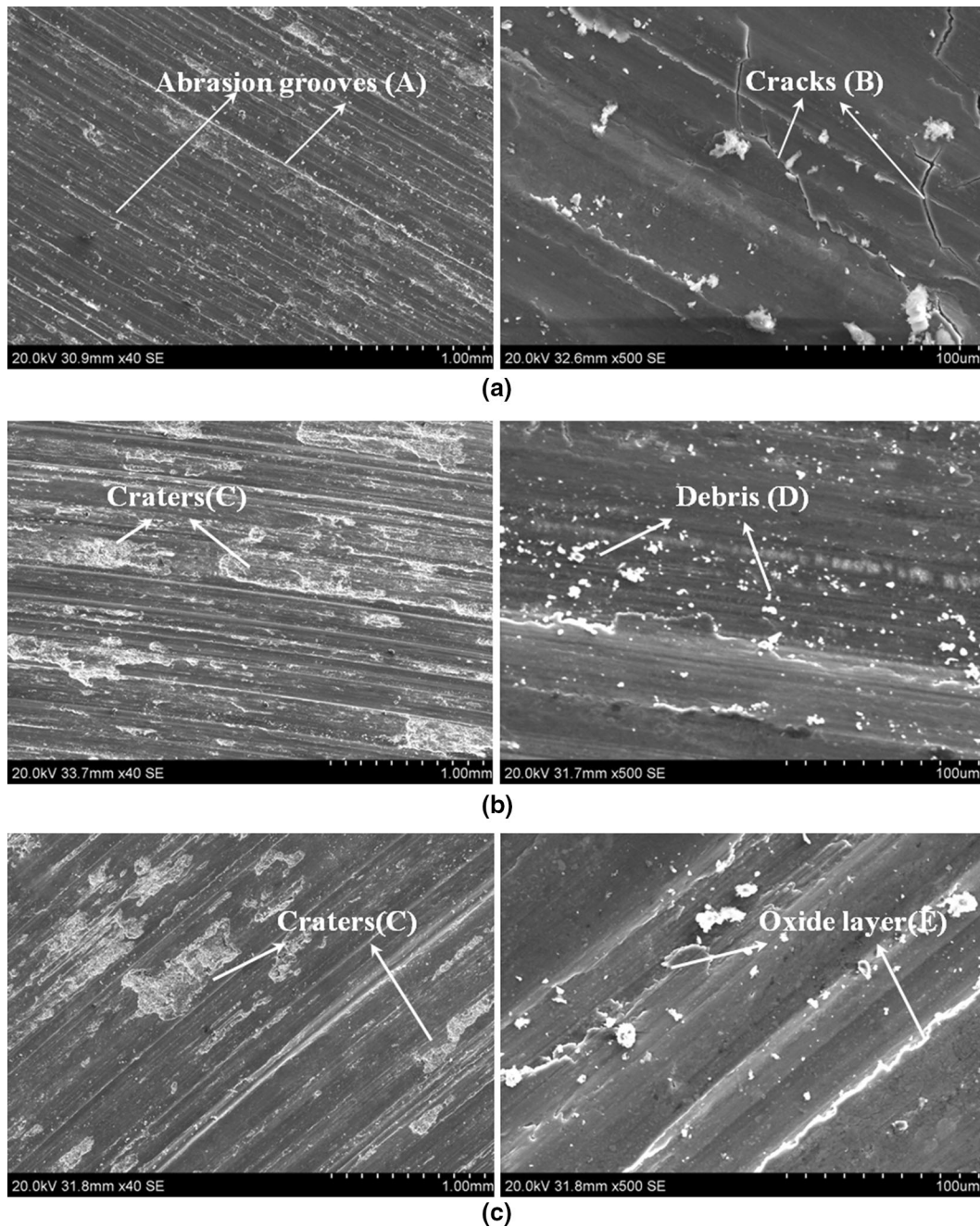
Fig. 13—SEM Micrographs of wear pins worn out surfaces of (*a*) 10-FGM inner region pin at 30 mm, (*b*) 15-FGM outer pin at 75 mm, and (*c*) 15-FGM inner pin at 30 mm, at 4 kg load condition.

particle-rich zones at different loads are shown in Figure 12. Even at the maximum load, only abrasion grooves are visible indicating mild wear as the prominent mechanism. For further understanding, the SEM images of worn-out surfaces of inner and outer FGMMC pins at 1 and 4 kg loading conditions are taken at different magnifications (Figures 13(a) through (c)). SEM analysis of pins shows the characteristic abrasion grooves, cracks, craters, debris, and oxide layers caused by abrasion wear mechanism.[28–30] The SEM micrograph of the worn surface reveals anchoring

of tribolayers at protruding SiC_p particles as well as the tribolayer delamination. The presences of protruding reinforcing particles at the worn-out surface indicate the existence of a strong reinforcement/matrix interface. SiC_p act as load-bearing elements in Al/SiCp composites, promoting the formation of a thick stable adherent tribolayers and improve the wear resistance. The formation of adherent tribolayer and its rate of formation will protect the aluminum matrix from wearing out. The SEM images show only a few delaminated particles, conforming the mild wear, even at high load. SEM

micrographs of wear tracks surfaces revealed that in mild wear conditions, the oxidized surface characteristics and scoring are the major wear mechanisms responsible for the material loss. Fine debris generated during the dry sliding have two contradictory roles. They may get locked between the sliding surfaces and promote the three body wears, which should enhance the volume loss in wear. In contrary, these oxide particles in the debris may be locked between the sliding surfaces and get compacted to form a protective hard transfer layer, so hard that there are no further scorings possible and in turn, it reduces the wear rate. Transfer layers can either adhere to the rubbing surfaces or flakes off from the surfaces, due to the micro-cutting and abrasion, during the dry sliding wear conditions.

IV. CONCLUSIONS

A319 Aluminum functionally graded metal matrix composites (FGMMC) reinforced with two different weight percentages SiC_p (10 and 15 wt pct) of average size 23 μm were processed successfully by liquid stir casting method followed by vertical centrifugal casting. The FGMMC microstructures reveal that centrifugal force has a greater influence in the formation of gradation in the system. The distribution curves of SiC_p reinforcements in the radial direction show that the position and magnitude of concentration of SiCp depend on percentage of initial addition. There is a shift of the position of maximum concentration towards the outer directions for higher percentage of additions. With a radial shift, from 55 to 75 mm, for 15-FGM, the maximum of 28 wt pct SiC_p is obtained. The density maximum of 2.87 g/cm^3 along with the lowest CTE value of 20.1 μm/mK is also obtained in the particle-rich zone of 15-FGM casting. Similarly, the hardness and ultimate tensile strength show a graded nature in correlation with particle concentration and are higher at particle-rich region. The maximum compressive strength of 15-FGM is 650 MPa in the particle-rich region. The wear resistance is higher in the particle-rich region of the FGMMC. The dry pin on disk wear test confirms that the mild wear is the major wear mechanism responsible for wear losses in these FGMMC castings.

REFERENCES

1. A. Mortensen and S. Suresh: *Int. Mater. Rev.*, 1995, vol. 40, pp. 239–65.
2. V.R. Rajeev, D.K. Dwivedi, and S.C. Jain: *4th International Conference on Recent Advances in Composite Materials, ICRACM-2013*, Varanasi, 18–21 February, 2013.
3. Y. Wanatanab and H. Sato: *Materials*, 2009, vol. 2, pp. 2510–25.
4. B. Kieback, A. Neubrand, and H. Riedel: *Mater. Sci. Eng. A*, 2003, vol. 62, pp. 81–105.
5. Yoshimi. Watanabe and Shin. Oike: *Acta. Mater.*, 2005, vol. 53, pp. 1631–41.
6. G. Chirita and I. Stefanescu: *Anales de Mecánica de la Fractura*, 2006, vol. I, pp. 317–22.
7. T.P.D. Rajan, R.M. Pillai, and B.C. Pai: *Mater. Charact.*, 2010, vol. 61, pp. 923–28.
8. Y. Watanabe, N. Yamanaka, and Y. Fukui: *Composites Part A*, 1998, vol. 29A, pp. 595–601.
9. O. Carvalho, M. Buciumeanu, S. Madeira, D. Soares, F.S. Silva, and G. Miranda: *Mater. Des.*, 2015, vol. 80, pp. 163–73.
10. A.G. Arsha, E. Jayakumar, T.P.D. Rajan, V. Antony, and B.C. Pai: *Mater. Des.*, 2015, vol. 88, pp. 1201–09.
11. Xuedong. Lin, Changming. Liu, and Haibo. Xiao: *Composites Part B*, 2013, vol. 45, pp. 8–21.
12. S. Kumar, V.S. Subramaniya, and B.S. Murty: *Metall. Mater. Trans. A*, 2010, vol. 41 (1), pp. 242–54.
13. R. Kayikci and Ö. Sava: *J. Compos. Mater.*, 2015, vol. 49 (16), pp. 2029–37.
14. S.L. Pramod, S.R. Bakshi, and B.S. Murty: *J. Mater. Eng. Perform.*, 2015, vol. 24 (6), pp. 2185–2207.
15. C. Saravanan, K. Subramanian, V.A. Krishnan, and R.S. Narayanan: *Mech. Mech. Eng.*, 2015, vol. 19 (1), pp. 23–30.
16. H. Kala, K.K.S. Mer, and S. Kumar: *Procedia Mater. Sci.*, 2014, vol. 6, pp. 1951–60.
17. M.O. Bodunrin, K.K. Alaneme, and L.H. Chown: *J. Mater. Res. Technol.* 2015, vol. 4(4), pp. 434–45.
18. M.C.G Shankar, P.K. Jayashree, R. Shetty, A. Kinia, and S.S. Sharma: *Int. J. Curr. Eng. Technol.*, 2013, vol. 3(3), pp. 922–34.
19. A. Halvaeea: Talebib*J. Mater. Process. Technol.*, 2001, vol. 118, pp. 123–27.
20. Y. Watanabe and A. Kawamoto: *Compos. Sci. Technol.*, 2002, vol. 62, pp. 881–88.
21. K.R. Ravi, V.M. Sreekumar, R.M. Pillai, C. Mahato, K.R. Amaranathan, R. Arul kumar, B.C. Pai: *Mater. Des.*, 2007, vol. 28, pp. 871–881.
22. E. Jayakumar, J.C. Jacob, T.P.D. Rajan, M.A. Joseph, B.C. Pai: *Mater. Sci. Forum*, 2015, vol. 830–831, pp. 456–459.
23. J. Gauthier, P.R. Louchez, and F.H. Samuel: *Cast Met.*, 1994, vol. 8 (2), pp. 91–106.
24. Z. Humberto and K. Sridharan: Melgarej*Composites Part A*, 2008, vol. 39, pp. 1150–58.
25. Z. Li, A.M. Samuel, F.H. Samuel, C. Ravindran, S. Valtierra, and H.W. Doty: *AFS Trans.*, 2003, vol. 2, pp. 241–54.
26. P.N. Crepeau: *AFS Trans.*, 1995, vol. 103, pp. 361–66.
27. J. Barresi, M.J. Kerr, H. Wang, and M.J. Couper: *AFS Trans.*, 2000, vol. 114, pp. 563–70.
28. D.K. Dwivedi: *Mater. Des.*, 2010, vol. 31, pp. 2517–31.
29. R.L. Deuis, C. Subramanian, and J.M. Yellup: *Compos. Sci. Technol.*, 1997, vol. 57, pp. 415–35.
30. V.R. Rajeev, D.K. Dwivedi, and S.C. Jain: *Mater. Des.*, 2010, vol. 31, pp. 4951–59.